

Title Finite element analysis of coating adhesion
failure in pre-existing crack field
Author(s) Holmberg, Kenneth; Laukkanen, Anssi;
Ronkainen, Helena; Wallin, Kim
Citation Tribology - Materials, Surfaces and Interfaces.
Maney Publishing. Vol. 7 (2013) No: 1 , Pages 42 - 51
Date 2013
URL <http://dx.doi.org/10.1179/1751584X13Y.0000000030>
Rights Post-print version of the article. This article may be
downloaded for personal use only.

<p>VTT http://www.vtt.fi P.O. box 1000 FI-02044 VTT Finland</p>	<p>By using VTT Digital Open Access Repository you are bound by the following Terms & Conditions.</p> <p>I have read and I understand the following statement:</p> <p>This document is protected by copyright and other intellectual property rights, and duplication or sale of all or part of any of this document is not permitted, except duplication for research use or educational purposes in electronic or print form. You must obtain permission for any other use. Electronic or print copies may not be offered for sale.</p>
---	---

FINITE ELEMENT ANALYSIS OF COATING ADHESION FAILURE IN A PRE-EXISTING CRACK FIELD

Kenneth Holmberg, Anssi Laukkanen, Helena Ronkainen, Kim Wallin
VTT Technical Research Centre of Finland, Espoo, Finland

Abstract

The influence of a pre-existing crack field on coating adhesion failure in a steel surface coated with a 2 micrometre thick titanium nitride (TiN) coating was investigated by finite element method (FEM) modelling and simulation. The stress and strain fields were determined in contact conditions with a spherical diamond tip sliding over the coated surface at a loading of 8 N. One crack in or at the coating increased the maximum tensile stresses with 6 times from 82 MPa to 540 MPa when the crack was vertical through the coating or L-shaped and with 9 times when the crack was horizontal at the coating/substrate interface. A simulated multicrack pattern relaxed the tensile stresses compared to single cracks. The results indicate that a cracked coated surface needs to have about 5-9 times higher adhesive and cohesive bonds to resist the same loading without crack growth compared to a crack free surface. For optimal coated surface design the strength of the adhesive bonds between the coating and the substrate in the vertical direction need to be 50% higher than the cohesive bonds within the coating and the substrate in the horizontal direction. The first crack is prone to start at the top of the coating and grows vertically down to coating/substrate interface and there it stops due to the bigger cohesion within the steel material. After this there are two effects influencing that the crack will grow in the lateral direction. One is that steel cohesion is normally bigger than coating/interface adhesion and the second is that there are higher tensile stresses in horizontal cracks than in vertical cracks. Several vertical cracks can stop the horizontal crack growth due to stress relaxation.

Keywords

Coating, fracture, scratch test, finite-element method, crack

1. Introduction

There has been an increased interest in surface engineering during the last few decades. This is much due to the rapid development in the coating deposition techniques. Today it is possible to coat a surface by various techniques with almost any material. A thin layer on the surface can drastically change the friction and wear properties of the surface. A layer of a few micrometre titanium nitride can increase the lifetime of cutting tools with two orders of magnitude and a similarly thin hard diamond-like carbon layer can reduce the coefficient of friction between two sliding metal surfaces to be fifty times lower, down to values as low as 0.01. This development has recently been reviewed by Holmberg and Matthews [1].

However, in certain conditions there are still problems with the reliability of coated components and there may occur cracks in the coatings resulting in unwanted wear. For this reason it is important to better understand the stresses and strains generated in loaded thin hard coatings, how they result in cracks on and close to the surface and how the cracks grow to form wear debris and generate wear. A crack perpendicular to the surface is often the start of the wear process and cracks that break the adhesive bonds in the interface between the coating and the substrate result easily in delamination of the coating.

The strength of the adhesive bonds between the coating and the substrate are crucial for the functionality of a coated surface. When they break, some part of the coating will be detached and the substrate material is exposed to the counter surface in the tribological contact. This is frequently called adhesive failure, coating delamination, spalling or flaking. The adhesive failure of a coated surface is basically that the moving counterface results in a pulling force at the surface, tensional stresses higher than what the material can resist and a crack is formed often in the interface between the coating and the substrate. The crack grows and merges with vertical through-coating cracks and a coating material flake is liberated and removed.

The adhesion strength between the coating and the substrate is governed by various routes for crack propagation depending on the elasticity, plasticity and ductility of the coating and the substrate and the coating thickness, and finally, typically results in spalling or buckling failure [2-4]. In practical systems it is not always clear if a failure at the coating/substrate interface is a truly adhesive failure or a cohesive failure in the coating or in the substrate along and very close to the interface. So in reality cohesive failures at the subinterface between the bulk material and the real interface to the coating are often referred to as adhesive failures [5]. Even if the theoretical definition of adhesion is clear, the assessment of adhesion is very difficult. This is reflected by the fact that there have been reported more than 350 different tests used to characterise adhesion [6-7].

Adhesion between the coating and the substrate is one important parameter but it cannot alone explain the interfacial properties. Other parameters such as geometry, applied and residual stresses and interfacial flaws are equally important. The well established field of fracture mechanics permits these aspects to be considered. One of the most important features of fracture mechanics is that it can provide means for characterising interfacial properties which does not depend on the method of testing [8-9].

Fracture near the surface often starts from imperfections in the material that form the nucleus for fracture initiation and propagation. Common imperfections are broken bonds on the interfaces, and inclusions, voids and dislocations in the layer. These imperfections have a disturbing effect on the stress field and the strains generated in the material.

Analytical solutions for coated surfaces with a flaw or a crack have been developed by a number of authors starting from Erdogan and Gupta [10-11] and reviewed by Hills et al. [12]. Many of the solutions are limited in use, because of the small number of cracks analysed, usually only one, and assumptions on the location of displacement zones along the crack faces.

An attempt to solve the problem of a spall more typical to those observed experimentally has been presented by Breton and Dubourg [13-14]. Using a half analytical and half numerical model based on the dislocation theory they simultaneously analysed the combination of an interfacial crack that propagates at the interface and a surface breaking crack that propagates normally to the interface. The energy release rate was determined at the crack tips. With the model they could show that the crack interaction favours propagation and that the surface breaking crack propagates down to the interface and the interfacial crack propagates at the interface in a direction opposite to that of the load displacement.

A theoretical model for multiple fatigue cracks situated close to a loading zone has been developed by Dubourg and Villechaise [15] and Dubourg et al. [16]. They considered straight arbitrarily oriented cracks and tested the method for up to five cracks without any indication of a limitation in crack number. For the analysis they identified five interaction mechanisms which depend on the distance between cracks, their relative position with respect to the loading zone, the interfacial crack coefficient of friction, and loading mode conditions: i.e. the step effect, the plug effect, the tilt effect, the stretch effect and the stretch-tilt effect.

The mechanisms of crack initiation and crack growth in surfaces covered by thin hard coatings and used in tribological contacts are not well understood. The problem is especially challenging for two reasons. The surface is a compound of a substrate and one or several layers having different material properties, and the dimensions of the layers, typically 0.5 to 5 μm , is four to five orders of magnitude smaller than the size range of the well-established linear elastic fracture mechanics concepts. Actually the dimension of the coating overlaps the size range, 0.1 – 1 μm , where material scientists normally define crack nucleation and initiation to take place [17].

There are some special features in the cracking of a surface covered by a thin coating. As a crack is initiated in a thin coating it normally goes all the way down to the coating/substrate interface. It may be only one single crack but often a whole system of cracks is generated [18]. When reaching the interface the crack may change direction and propagate along the coating/substrate interface or it may penetrate deeper down into the substrate. The crack growth in the lateral direction is important since it influences the conditions for coating delamination.

Analytical and numerical solutions of fully and partially cracked thin coatings in a stress field in tension and unstressed have been presented by Beuth [19], Menčík [20] and Oliveira and Bower [21]. Still the use of these solutions in practical applications is not easy and straightforward due to the mathematical complexity. Finite element modelling (FEM) was used by Rabinovich and Sarin [22] to show the mechanisms of fracture in brittle materials under scratch test sliding indentation loading. The study includes frictional contact interaction, crack propagation and debonding of laminated brittle three-dimensional finite bodies. They showed that the dominating mechanism of the interfacial debonding is different for coated and homogeneous surfaces.

In a FEM study of the interface cracking between a hard coating and a softer substrate in indentation Souza et al. [23] found that the interfacial cracks: (i) did not interact with the bending stresses responsible for the circular cracks observed close to the contact edge of indentations of coated systems

with soft substrates; (ii) reduced the constraints imposed by the substrate on the coating, which may be responsible for the propagation of the coating cracks during the unloading portion of the indentation; and (iii) resulted in an overall and localised reduction in the coating stresses in most portions of the model, which is important in areas close to the indentation axis, where a reduction in the amount of circular and radial cracks would be expected.

Surface cracking of a multilayered surface due to repeated sliding of a rigid asperity was analysed by linear elastic fracture mechanics and FEM by Gong and Komvopoulos [24-25]. They studied the propagation of a partial perpendicular crack in the first coating layer and came up with several very interesting conclusions. The significantly higher values, by an order of magnitude, of the tensile stress intensity factor, K_I , than those of the shear intensity factor, K_{II} , indicate that surface cracking in a multilayered surface due to sliding is controlled by the tensile fracture mode. Longer surface cracks produce significantly higher K_I values while higher friction increases both K_I and K_{II} significantly due to the strong effect of the surface shear traction on the crack-tip stresses. The increase of friction at the crack interface promotes stress relaxation but the effect on K_I is negligible. The initial crack growth was found to occur at an angle of $\sim 10^\circ$ from the original crack plane, independent of the initial crack length. After the first one to three crack growth increments, the crack growth paths are almost parallel to each other, exhibiting a common deviation from the original crack by $\sim 57^\circ$ and this was reported to be in fair agreement with experimental observations.

Laukkanen et al. [26] carried out a fracture mechanics evaluation of thin coated surfaces by boundary element analysis based on the stress and strain FEM analysis carried out by Holmberg et al. [27-28]. They analysed the fracture conditions in the contact of a rigid diamond sphere sliding with increased loading on a flat steel surface coated with a 2 μm thick TiN coating. In addition to calculating the first principal stresses on the top of the surface and at the coating/substrate interface they calculated the true stresses in tension and in shear. They found that the highest tensile stress levels are at the surface in the sliding direction and the direction perpendicular to sliding. This explains why the first cracks observed in these conditions are typically angular cracks at the groove edge behind the slider. It clearly indicates that the surface cracking starts from the top of the coating and advances down to the interface and into the substrate. They showed that the shear stress level is lower than the tensile stresses and that the highest shear stresses are generated on top of the coating in the surface plane.

Laukkanen et al. [26] further studied the influence of different crack parameters on crack growth by calculating the stress intensity factor, K , along the crack front. The tension mode I dominates the crack growth in lateral directions even if the shear mode II seems to be important for crack growth in the vertical direction. The influence from mode III is negligible in the analyses. From a crack parameter analysis they concluded that cracks vertical to the sliding direction are more prone to grow compared with cracks 20° and 45° from the vertical direction; cracks with a larger crack spacing in the regular crack field (30 μm) are more prone to grow compared to smaller spacing (5 and 10 μm) or single cracks; the centre crack in a crack field is more prone to grow compared to edge crack or other cracks in the field; transverse cracks in the middle of the groove are more prone to grow compared to both transverse and angular side cracks at the groove edge; and tensile load biaxiality has only a marginal influence on crack growth.

In ceramic coatings the thickness and the grain size are important parameters for crack propagation. In indentation tests of 1 to 10 μm thick Al_2O_3 coatings on cemented carbide substrates Yuan and Hayashi [29] found that the critical load for generation of radial cracks decreased with increasing coating thickness and that the grain size of the coatings decreased with the thickness. A coarser grained microstructure generally displays a lower cohesive strength as compared with a fine grained

microstructure. Thus the fracture strength of the coating increases with decreasing grain size and decreasing thickness.

For amorphous diamond-like carbon (DLC) coatings in the thickness range of 0.7 to 2 μm it has been shown that the hardness and apparent fracture toughness of the coating/substrate combination, measured by Vickers indentation, depend on the thickness of the coating [30]. The hardness and the apparent fracture toughness of the coating, both of which influence the wear, increased with increasing coating thickness. The hardness and the thickness influenced the initiation of cracks, whereas the residual stress in the film influenced the propagation of cracks.

In a study of very thin DLC coatings in the thickness range of 3.5 to 20 nm Sundarajan and Bhushan [31] conclude that the formation of cracks depends on the hardness and fracture toughness of the coating. They suggest that the observed non-uniform failure depends on variations in the coating properties at different locations in the material volume. Surface cracks are developed in weaker regions with lower fracture toughness. As cracks propagate they are forced to expand within the weak region, as the neighbouring strong regions inhibit extensive lateral crack growth. Because of this, cracks propagate down to the interface, where, aided by the interfacial stresses, they get diverted along the interface just enough to cause local delamination of the coating. Simultaneously the weakened regions experience excessive ploughing. Thus weaker regions fail while stronger regions remain wear-resistant. The propagation of cracks along the coating/substrate interface is suppressed due to the strong adhesion of the coating; otherwise would coating delamination take place.

The objective of our recent research work has been to develop a method for optimising the mechanical properties of a coated surface to be used in tribological contacts with respect to surface fracture [26-28;32-35]. In our studies we have used a fracture mechanics approach and studied the contact condition of a sphere sliding over a surface coated with a thin hard coating. A three dimensional finite-element method (3D FEM) model has been developed for calculating the first principal stress, true stress, true shear and strain distributions, and parameters influencing the crack propagation in the contact of the spherical tip moving with increased load on a coated steel surface. The used 3D FEM model was in our previous studies compared with empirical observations and the correlation was good and encouraging. The purpose of this paper is to demonstrate with a 2D FEM model and stress and strain computer simulations the effect of single and multiple perpendicular cracks going straight through the coating and lateral cracks in the interface between the coating and the substrate both separately and combined in the pre-existing crack field.

2. Surface parameters

The modelled contact condition is a ball sliding over a flat coated surface, as shown in *figure 2.1*. The materials are homogenous and the surfaces perfectly smooth. The two dimensional simulation figures shown in this paper are in the vertical symmetry plane along the direction of sliding.

The parameters used in the simulations are the following:

- the substrate is high speed steel (HSS) with hardness $H = 7.5$ GPa; Young's modulus $E = 200$ GPa; Poisson's ratio $\nu = 0.29$; strain hardening coefficient = 20; and yield strength = 4100 MPa,
- the coating is titanium nitride (TiN) with a thickness of $h = 2$ μm ; hardness $H = 25$ GPa; Young's modulus $E = 300$ GPa; and Poisson's ratio $\nu = 0.22$,
- the adhesion between the coating and the substrate outside the cracks is 100%,
- the sliding tip is diamond and thus modelled as rigid with a radius of $R = 200$ μm ,

- the sliding condition corresponds to a scratch test situation with 8 N (4.5 N/mm) normal load and
- the coefficient of adhesive friction between the tip and the coated surface is $\mu = 0.08$.

3. Surface crack model

The finite element analyses were carried out using the Warp3D [36] and Abaqus [37] general purpose finite element software. The contact problem is treated as a finite deformation and finite sliding analysis, where a linear-elastic tip slides above the linear-elastic coating and elastic-plastic substrate layers with boundary conditions corresponding to those specified in Chapter 2 for a typical scratch test. The basis for constructing the finite element mesh is such that using non-adaptive means cracking within the coating as well as at the coating-substrate interface can be modeled incrementally at a certain point of sliding, as presented in Figure 3.1. In order to achieve this, the mesh topology is designed such that allowance is made for through coating cracking during the scratch test followed by a dense region where crack propagation also at the interface, thus representing the adhesive failure process, is included. Mesh detail with details of various cracks is presented in Figure 3.2.

In order to study the system's behavior during different cracking processes, several different crack growth variations are studied. These are the: i) non-cracking, ii) through coating cracking, iii) adhesive interface cracking, iv) through coating and interface cracking, and v) through coating cracking crack field and interface cracking cases. By generating the different analysis variants the resulting differing fields of stress and strain can be assessed. The mesh construct between the different cases is essentially similar in terms of density and near crack-tip seeding.

The crack initiation and propagation process takes place in a linear-elastic material and during a minute change in the external boundary conditions of the system. The crack propagation process is specified to occur following a pre-defined path at an instance of loading identified on the basis of previous experimental and numerical work once the contacting tip has slid over the failing region, i.e. the failure initiates once the coating has resurfaced from under the contact [26-28;38]. The actual critical occurrence is specified to correspond to mean fracture toughness values determined in [26] for through coating cracks which were observed experimentally and the fracture toughness estimated on the basis of numerical means. Thus, the following crack propagation takes place via a node release approach, where once certain free surface has been created, following iterations are carried out in order for the FEM model to reach equilibrium, after which subsequent crack propagation can occur. The process is carried out repeatedly - typically for several tens of steps - until the desired crack geometry has been reached. The crack field density in the analyses where the interface crack growth is preceded by through coating cracking is as well specified on the basis of [26].

The FEM model is a 3D model with dimensions $5000 \mu\text{m} \times 250 \mu\text{m} \times 250 \mu\text{m}$ (length in sliding direction \times width \times depth), and half model symmetry is imposed. The dimensions are selected such that undesired interaction between the system boundary conditions and the area undergoing contact finite strain plasticity are avoided. Element sizing of bilinear isoparametric 3D brick elements ranges from 10 nm upwards. Kinematic incremental plasticity formulation is applied, and a Coulomb friction model with a constant coefficient of friction. Contact is enforced using a penalty function approach. Figures 4.1-4.5 are 2D symmetry plane images of simulations carried out with the 3D model.

4. Stress and strain simulation results

The stresses and strains in the coated surfaces below the sliding tip as the tip slides from left to right for the five cases with and without pre-existing cracks are shown in figures 4.1 - 4.5. The position of the sliding tip is in all figures above the blue compressive stress area at the surface on the right hand side of the crack field.

4.1 Surface without cracks

The stresses and strain in the coated loaded surface were first simulated for a surface with no pre-existing cracks, as shown in figure 4.1. In figure 4.1a are the first principal stresses illustrated with a maximum compression of 1013 MPa at the surface and maximum tensile stresses of 82 MPa at the coating/substrate interface below the sliding tip. The position of the tip is above the blue compressive zone and the extension of the contact zone is about 3 μm in diameter. Figure 4.1b shows that the maximum strain reaches a value of 0.2 % at the substrate/coating interface and figure 4.3c shows the shear pattern and the maximum shear stresses of values up to 304 MPa. The pure tensile stresses in the vertical direction are shown in figure 4.1d.

4.2 Surface with one vertical crack

The stresses and strain were in this case simulated in a similar coated loaded surface but now with one vertical pre-existing crack going all the way through the 2 μm thick coating, as shown in figure 4.2. In figure 4.2a are the first principal stresses illustrated with a maximum compression concentration of 1061 MPa just under the sliding tip and a maximum tensile stress concentration of 541 MPa on the trailing side at the crack edge. The maximum compressive stress at the tip edge is 1851 MPa. Figure 4.2b shows the large maximum strain pattern with values above 0.2 % on the right hand side of the crack and figure 4.2c shows the shear pattern and the maximum shear stresses of values up to 588 MPa just at the crack edge. The pure tensile stresses in the vertical direction are shown in figure 4.2d.

4.3 Surface with one horizontal crack

The stresses and strain were in this case simulated in a similar coated loaded surface but now with one horizontal pre-existing 1 μm long crack in the substrate/coating interface, as shown in figure 4.3. In figure 4.3a are the first principal stresses illustrated with a maximum compression concentration of 970 MPa under the sliding tip and small compressive stress concentrations just at both crack edges, the one on the trailing side being higher 1096 MPa. A maximum tensile stress concentration of 765 MPa is found on the coating side of the crack. Figure 4.3b shows the strain pattern with maximum strain values above 0.2 % on both sides of the crack and figure 4.3c shows the shear pattern and the maximum shear stresses of values up to 391 MPa. The pure tensile stresses in the vertical direction are shown in figure 4.3d.

4.4 Surface with L-shaped crack

The stresses and strain were in this case simulated in a similar coated loaded surface but now with an L-shaped pre-existing crack going all through the 2 μm thick coating and continuing with a 1 μm long crack going horizontally along the substrate/coating interface, as shown in figure 4.4. In figure

4.4a are the first principal stresses illustrated with a maximum compression concentration of 942 MPa under the sliding tip and another compression stress concentrations just at edge of the horizontal crack and at the crack corner, both reaching very high values of up to 3754 MPa. Minor tensile stress concentrations are found on both sides of the horizontal crack and at the vertical crack close to the crack corner not being much more than 537 MPa. Figure 4.4b shows the strain pattern with maximum strain values above 0.2 % especially at the crack edge and crack corner and figure 4.3c shows the shear pattern and the maximum shear stresses of values of 1098 MPa at the inner corner. The pure tensile stresses in the vertical direction are shown in figure 4.4d.

4.5 Surface with several vertical and one L-shaped crack

The stresses and strain were in this case simulated with the most complicated pre-existing crack pattern. A similar coated loaded surface as above had now 10 vertical cracks going straight through the 2 μm thick coating and one of them being L-shaped and continuing with a 1 μm long crack going horizontally along the substrate/coating interface, as shown in figure 4.5. In figure 4.5a are the first principal stresses illustrated with a maximum compressive stress concentration of 967 MPa under the sliding tip and two other compressive stress concentrations just at the crack corner of the L-shaped crack and at its horizontal crack edge, both reaching very high values of up to 3697 MPa. Minor tensile stress concentrations are found on both sides of the horizontal crack and at the vertical crack close to the crack corner not being much more than 420 MPa. Figure 4.5b shows the strain pattern with maximum strain values above 0.2 % especially at the crack edge and crack corner of the L-shaped crack and figure 4.3c shows the shear pattern and the maximum shear stresses of values of up to 1118 MPa at the inner corner. The pure tensile stresses in the vertical direction are shown in figure 4.5d.

The simulated stress and strain results in the five different crack pattern cases are summarised in table 4.1 below.

Table 4.1 Summary of stress and strain maximum values for the five simulated cases. Global top values are highlighted with bold.

	Crack-free surface	One vertical crack	One horizontal crack	One L-shaped crack	Multiple crack pattern
Max compression stress under tip (MPa)	-1013	-1061	-970	-942	-967
Max compression stress at crack tip or corner (MPa)	-	-1851	-1096	-3754	-3697
Max tensile first principal stress (MPa)	82	541	765	537	420
Area (μm^2) where strain in is exceeding 0.2%	1.4	8.3	3.3	4.4	3.3
Max shear stress (MPa)	304	-588	-391	-1098	-1118
Max tensile stress in vertical direction (MPa)	2	519	36	463	49

5. Discussion

The simulated stress and strain results give us the possibility to analyse the influence of different pre-existing cracks and crack patterns in a coated surface. Below we analyse the changes in material

stresses and strain due to the pre-existing cracks compared to a crack free coated surface. The comparison is done both quantitatively by comparing maximum compressive and tensile stresses and strain and qualitatively by comparing the stress and strain pattern in the coated surface and around the cracks. Special attention is given to the tensile stresses since they have a crucial effect of the crack growth and thus on the generation of material completely surrounded by cracks and resulting in wear particles.

Based on quantitative stress and strain values (table 4.1) and patterns (figures 4.1-4.5) simulated for the five different crack cases can the following observations be recorded. They show that one single vertical or horizontal crack in the coating does not have much influence on the maximum compressive stresses at the surface under the tip. The compressive stresses under the tip are increased with 5% by a vertical crack but decreased by about 5% by a horizontal, an L-shaped or a multi+L-shaped crack pattern.

A single vertical crack through the coating increases the maximum tensile stresses to 6 times higher values compared to a crack free surface while a single horizontal crack at the substrate/coating interface increases the maximum tensile stresses to 9 times higher values compared to a crack free surface. High tensional stress concentrations occur along the sides of the horizontal cracks at the substrate/coating interface.

Very high compressive stress concentrations occur at the crack edge and at the corner of the L-shaped crack and the multi+L-shaped cracks. This shows that one horizontal crack has some load carrying capacity resulting in 1096 MPa maximum compressive stresses. One vertical crack has a decreased load carrying capacity resulting in 1851 MPa maximum compressive stress. The L-shaped and multi+L-shaped crack fields have very poor load carrying capacity resulting in compressive stress peaks as high as 3700-3750 MPa. A multicrack pattern like the studied multi+L-shaped has 45% lower maximum tensile stresses compared to a surface with one single horizontal crack.

The maximum shear stresses are increased from 304 MPa with 30% when one single horizontal crack is introduced, with 90% when one single vertical crack is introduced and with 250% up to values of about 1100 MPa when L-shaped or multi+L-shaped crack fields are introduced.

The cross sectional area where 0.2% of strain is exceeded corresponds to the extent of the plastic deformation. This is 6 times larger with one vertical crack compared to the crack free surface and 2-3 times larger in the other crack pattern cases studied. This illustrates the relaxation taking place at the surface. The highest volume of plasticity with one vertical crack is explained by two effects; one is that the coating has a through crack and does not carry the load, and the second is that there is no relaxation by multiple cracks.

The tensile stresses in vertical directions are close to zero in a crack free coated surface. One horizontal crack does not much change the stress field. One vertical crack on the other hand results in high vertical stresses due to compression on the tip side of the crack. The same compression is observed with the L-shaped crack but it is lower due to some relaxation from the horizontal crack part. The vertical stresses are again close to zero with the multi+L-shaped crack field due to relaxation.

The qualitative analysis of the different pre-existing crack patterns in the coated surface show big changes in the stress and strain concentrations. One vertical crack going through the coating brings a high compressive stress concentration on the loading side of the crack edge where the material is

pushed down and a high tensile stress concentration on the trail side of the crack close to the crack edge. Considerable strain occurs in a large material volume on the loaded side of the crack edge and very high shear stresses occur close to the crack edge.

One horizontal crack at the substrate/coating interface brings very high tensile stresses on both the upper and lower side of the horizontal crack and this will crucially influence on the crack growth. Optimisation of the material parameters in the coating system should focus on reducing these tensile stresses to result in a surface with good cracking and wear resistance.

An L-shaped crack brings very high compressive stress concentrations as well as high tensile stress concentrations close to the crack edge and corner while multiple vertical cracks in addition to the L-shaped crack result in some stress relaxation and reduce the stress levels.

Beneficial relaxation of tensile stresses can be observed for L-shaped and multi+L-shaped crack fields but at the same time there is a considerable increase in the shear stresses which may result in adhesive interface cracking and failure.

The length of the pre-existing cracks was not varied in this study but, according to the authors experience and understanding, it is not expected that the length difference of the lateral and vertical cracks has much effects on the analysis because even the shorter crack resides the highly stressed region.

In a loaded contact like the simulated one the first crack is prone to start at the top of the coating and grows vertically down to coating/substrate interface and there it stops due to the bigger cohesion within the steel material [27]. After this there are two effects influencing that the crack will grow in the lateral direction. One is that steel cohesion is normally bigger than coating/interface adhesion and the second is that there are higher tensile stresses in horizontal cracks than in vertical cracks.

6. Conclusions

The influence of a pre-existing crack pattern on the stresses and strain in a steel surface coated with a 2 μm thick TiN coating was studied. The coated surface was loaded by a sliding 200 μm radius diamond tip with a load of 8 N. A crack free coated surface resulted in 82 MPa max tensile stresses occurring at the substrate/coating interface in the simulated loading conditions.

One crack in or at the coating increased the tensile stresses with 6 times up to 540 MPa when the crack was vertical through the coating or L-shaped and with 9 times up to 765 MPa when the crack was lateral at the coating/substrate interface. The simulated multicrack pattern relaxed the tensile stresses down to below 420 MPa.

The results indicate that for optimal coated surface design the strength of the adhesive bonds between the coating and the substrate in the vertical direction need to be 50% higher than the cohesive bonds within the coating and the substrate in the horizontal direction. A cracked coated surface needs to have about 5-9 times higher adhesive and cohesive bonds to resist the same loading without crack growth compared to a crack free surface.

When several vertical cracks have been created they may stop the horizontal crack growth due to considerable stress relaxation.

Acknowledgement

The financial support of TEKES the Finnish Technology Agency; Savcor Coatings, Finland; and the VTT Technical Research Centre of Finland is gratefully acknowledged.

References

- (1) Holmberg K, Matthews A. Coatings Tribology – Properties, Mechanisms, Techniques and Applications in Surface Engineering. 2nd ed. Tribology and Interface Engineering Series 56. Amsterdam: Elsevier; 2009.
- (2) Swain MV, Menčík J. Mechanical property characterization of thin films using spherical tipped indenters. *Thin Solid Films* 1994; 253: 204-211.
- (3) Bull SJ. Failure mode maps in the thin film scratch adhesion test. *Tribology Int.* 1997; 30:491-498.
- (4) Diao D, Kandori A. Finite element analysis of the effect of interfacial roughness and adhesion strength on the local delamination of hard coating under sliding contact. *Tribology Int.* 2006;39:849-855.
- (5) Malzbender J, Den Tooder JMJ, Balkenende AR, De With G. Measuring mechanical properties of coatings: a methodology applied to nano-particle-filled sol-gel coatings on glass. *Materials Science and Engineering* 2002; R36:47-103.
- (6) Mittal KL (ed). Adhesion measurement of films and coatings. Utrecht, The Netherlands: VSP; 1995.
- (7) Mittal KL (ed). Adhesion measurement of films and coatings. Vol. 2. Utrecht, The Netherlands: VSP; 2001.
- (8) Thouless MD. The role of fracture mechanics in adhesion. MRS Materials Research Society Symp., March 1988, Reno, Nevada, USA, Proc. 1988;119:51-62.
- (9) Venkatamaran SK, Nelson JC, Hsieh AJ, Kohlstedt DL, Gerberich WW. Continuous scratch test measurements of thin film adhesion strengths. In: Adhesion Measurement of Films and Coatings, Mittal, K.L. (ed.), Utrecht, The Netherlands: VSP; 1995;161-174.
- (10) Erdogan F, Gupta GD. Layered composites with an interface flaw. *Int. J. Solids Structures* 1971a;7:1089-1107.
- (11) Erdogan F, Gupta GD. The stress analysis of multi-layered composites with a flaw. *Int. J. Solids Structures* 1971b;7:39-61.
- (12) Hills DA, Nowell D, Sackfield A. A survey of cracks in layers propelled by contact loading. In: Mechanics of coatings. Dowson, D. & al. (eds) Tribology series 17. Amsterdam: Elsevier; 1990;203-208.
- (13) Breton E, Dubourg MC. Adhesion for coatings. 18th Leeds-Lyon Symp. on Tribology, 3-6.9.1991, Lyon, France, Elsevier Tribology Series No 21. Amsterdam: Elsevier; 1991a;41-47.
- (14) Breton E, Dubourg MC. Behaviour of cracked coating submitted to Hertzian moving contact. 18th Leeds-Lyon Symp. on Tribology, 3-6.9.1991, Lyon, France, Elsevier Tribology Series No 21. Amsterdam: Elsevier; 1991b.
- (15) Dubourg MC, Villechaise B. Analysis of multiple cracks - Part I: Theory. *J. of Tribology, Trans. ASME* 1992;114:455-461.
- (16) Dubourg MC, Godet M, Villechaise B. Analysis of multiple fatigue cracks - Part II: Results. *J. of Tribology, Trans. ASME* 1992;114:462-468.
- (17) Miller KJ. The short crack problem. *Fatigue of Engineering Materials and Structures* 1982;5:223-232.
- (18) Bull SJ. Failure modes in scratch adhesion testing. *Surface and Coatings Technologies* 1991;50:25-32.
- (19) Beuth JL. Cracking of thin bonded films in residual tension. *Int. J. Solids Structures* 1992;29:1657-1675.

- (20) Menčík J. *Mechanics of Components with Treated or Coated Surfaces*. London: Kluwer Academic Publishers, Solid Mechanics and its Applications Series vol. 42; 1996.
- (21) Oliveira SAG, Bower AF. An analysis of fracture and delamination in thin coatings subjected to contact loading. *Wear* 1996;198:15-32.
- (22) Rabinovich VL, Sarin VK. Modelling of interfacial fracture. *Materials Science and Engineering* 1996;A209:82-90.
- (23) Souza RM, Mustoe GGW, Moore JJ. Finite element modeling of the stresses, fracture and delamination during the indentation of hard elastic films on elastic-plastic soft substrates. *Thin Solid Films* 2001;392:65-74.
- (24) Gong ZQ, Komvopoulos K. Surface cracking in elastic-plastic multi-layered media due to repeated sliding contact. *Trans. ASME, J. Tribology* 2004;126:655-663.
- (25) Gong ZQ, Komvopoulos K. Contact fatigue analysis of an elastic-plastic layered medium with a surface crack in sliding contact with a fractal structure. *J. Tribology, Trans. ASME* 2005;127:503-512.
- (26) Laukkanen A, Holmberg K, Koskinen J, Ronkainen H, Wallin K, Varjus S. Tribological contact analysis of a rigid ball sliding on a hard coated surface - Part III: Fracture toughness calculation and influence of residual stresses. *Surface and Coatings Technology* 2006;200:3824-3844.
- (27) Holmberg K, Laukkanen A, Ronkainen H, Wallin K, Varjus S, Koskinen J. Tribological contact analysis of a rigid ball sliding on a hard coated surface - Part I: Modelling stresses and strains. *Surface and Coatings Technology* 2006a;200:3793-3809.
- (28) Holmberg K, Laukkanen A, Ronkainen H, Wallin K, Varjus S, Koskinen J. Tribological contact analysis of a rigid ball sliding on a hard coated surface - Part II: Material deformations, influence of coating thickness and Young's modulus. *Surface and Coatings Technology* 2006b;200:3810-3823.
- (29) Yuan F, Hayashi K. Influence of the grain size of the aluminium coating on crack initiation in indentation. *Wear* 1999;225-229:83-89.
- (30) Kodali P, Walter KC, Nastasi M. Investigation of mechanical and tribological properties of amorphous diamond-like carbon coatings. *Tribology Int.* 1997;30:591-598.
- (31) Sundararajan S, Bhushan B. Micro/nanotribology of ultrathin hard amorphous carbon coatings using atomic force/friction force microscopy. *Wear* 1999;225-229:678-689.
- (32) Holmberg K, Laukkanen A, Ronkainen H, Wallin K, Varjus S. A model for stresses, crack generation and fracture toughness calculation in scratched TiN-coated steel surfaces. *Wear* 2003;254:278-291.
- (33) Holmberg K, Ronkainen H, Laukkanen A, Wallin K, Erdemir A, Eryilmaz O. Tribological analysis of TiN and DLC coated contacts by 3D FEM modelling and simulation. *Wear* 2008;264:877-884.
- (34) Holmberg K, Laukkanen A, Ronkainen H, Wallin K. Surface stresses in coated steel surfaces - influence of a bond layer on surface fracture. *Tribology Int.* 2009a;42:137-148.
- (35) Holmberg K, Ronkainen H, Laukkanen A, Wallin K, Hogmark S, Jacobson S, Wiklund U, Souza R, Ståhle P. Residual stresses in TiN, DLC and MoS₂ coated surfaces with regard to their tribological fracture behaviour. *Wear* 2009b;267:2142-2156
- (36) WARP3D-Release 15.9, University of Illinois at Urbana-Champaign 2008.
- (37) ABAQUS, release 6.9-EF1, Simulia 2010.
- (38) Laukkanen A, Holmberg K, Ronkainen H, Wallin K. Cohesive zone modelling of initiation and propagation of multiple cracks in hard thin surface coatings, *Journal of ASTM Int.* 2010; available on web, paper ID102525.

Figure captions

Figure 2.1 The stress field in a coated surface resulting from a sliding sphere is a result of four loading effects: friction force, geometrical deformations, bulk plasticity concentration and residual stresses. Illustration (a) shows the loading effects with exaggerated dimensions and deformations and (b) with correct dimension interrelationships.

Figure 3.1 Adhesion cracking from pre-existing crack field of specific density.

Figure 3.2 Schematic illustration of the finite element mesh. The mesh sizing is in the range of **10 nm – 2 μm** and the number of mesh nodes is about **500k**.

Figure 4.1 Simulation of stresses and strains in a 2 μm thick TiN coating deposited on high speed steel plate **without any cracks** loaded by a 200 μm radius diamond tip under 8 N normal load. (a) First principal stresses, (b) strains, (c) shear stresses in the plane of the figure, and (d) tensile stresses in the vertical direction. The stress values on the scale are given as MPa.

Figure 4.2 Simulation of stresses and strains in a 2 μm thick TiN coating deposited on high speed steel plate **with one 2 μm vertical crack** loaded by a 200 μm radius diamond tip under 8 N normal load that just has passed over the cracked surface. (a) First principal stresses, (b) strains, (c) shear stresses in the plane of the figure, and (d) tensile stresses in the vertical direction. The stress values on the scale are given as MPa.

Figure 4.3 Simulation of stresses and strains in a 2 μm thick TiN coating deposited on high speed steel plate **with one 1 μm horizontal interface crack** loaded by a 200 μm radius diamond tip under 8 N normal load that just has passed over the cracked surface. (a) First principal stresses, (b) strains, (c) shear stresses in the plane of the figure, and (d) tensile stresses in the vertical direction. The stress values on the scale are given as MPa.

Figure 4.4 Simulation of stresses and strains in a 2 μm thick TiN coating deposited on high speed steel plate **with an L-shaped crack** loaded by a 200 μm radius diamond tip under 8 N normal load that just has passed over the cracked surface. (a) First principal stresses, (b) strains, (c) shear stresses in the plane of the figure, and (d) tensile stresses in the vertical direction. The stress values on the scale are given as MPa.

Figure 4.5 Simulation of stresses and strains in a 2 μm thick TiN coating deposited on high speed steel plate **with ten vertical and one L-shaped crack** loaded by a 200 μm radius diamond tip under 8 N normal load that just has passed over the cracked surface. (a) First principal stresses, (b) strains, (c) shear stresses in the plane of the figure, and (d) tensile stresses in the vertical direction. The stress values on the scale are given as MPa.

Table captions

Table 4.1 Summary of stress and strain maximum values for the five simulated cases. Global top values are highlighted with bold.

Figures

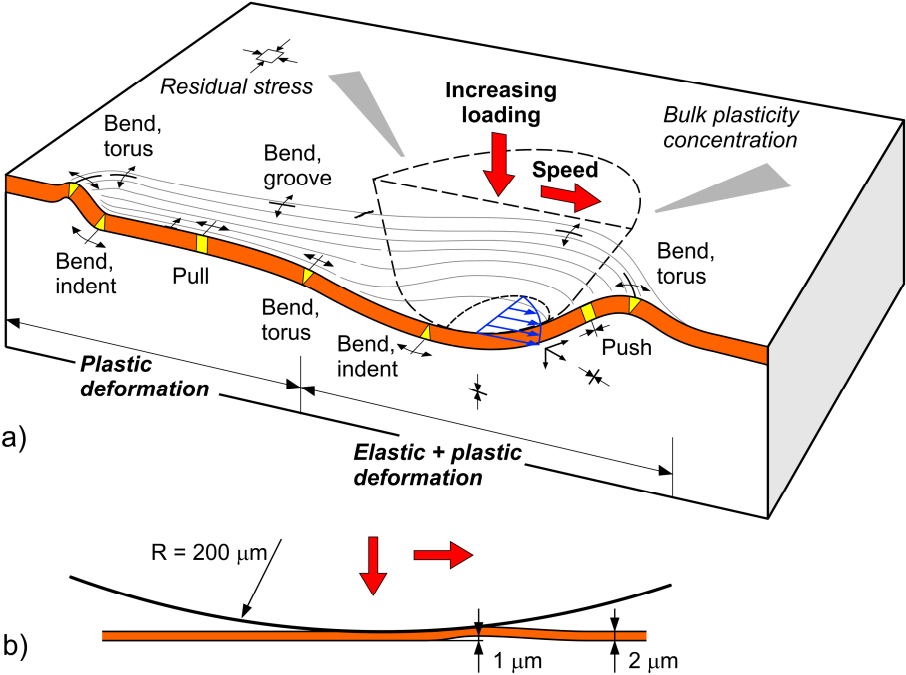


Fig. 2.1

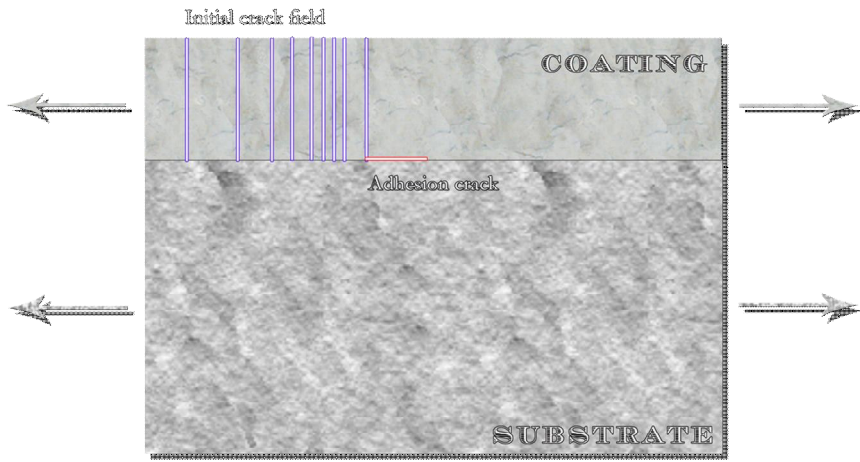


Fig. 3.1

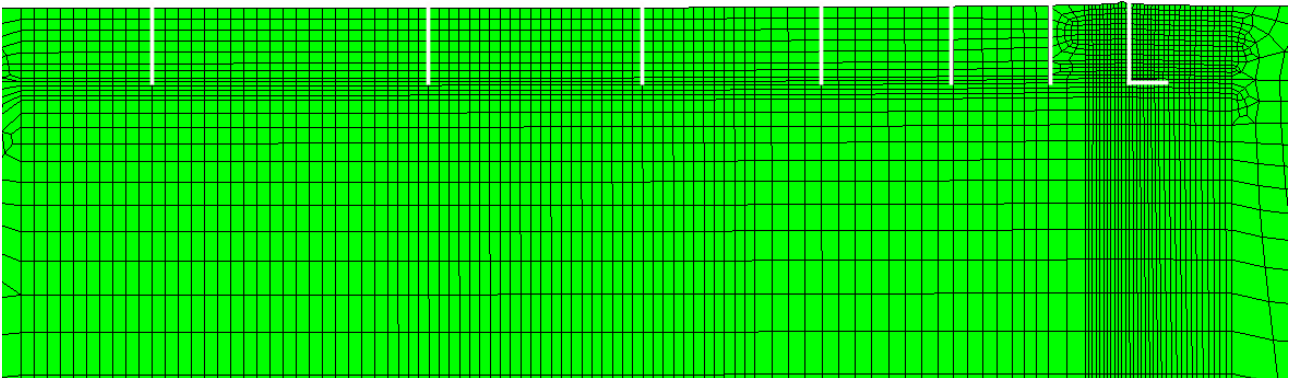
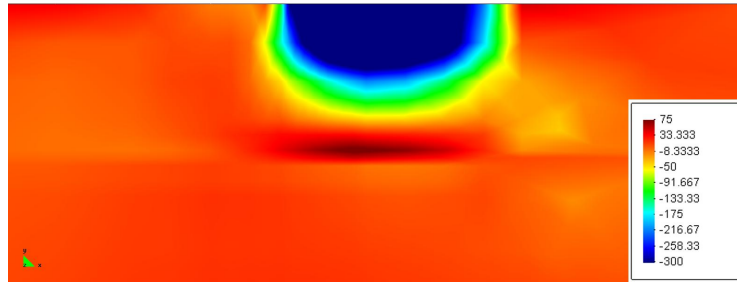
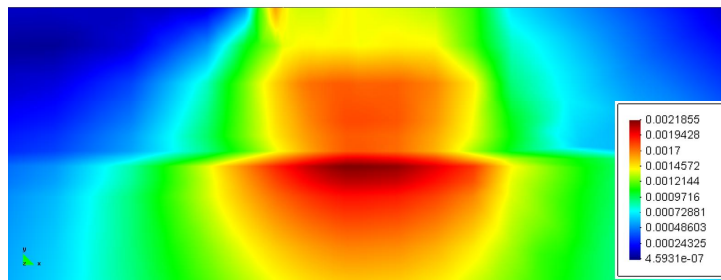


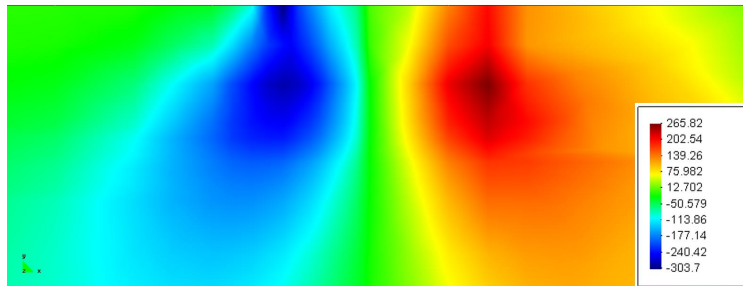
Fig. 3.2



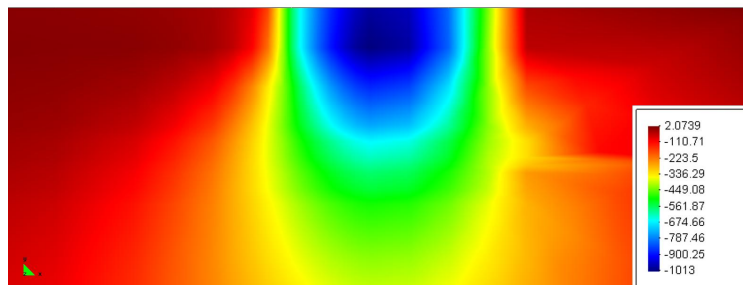
a



b

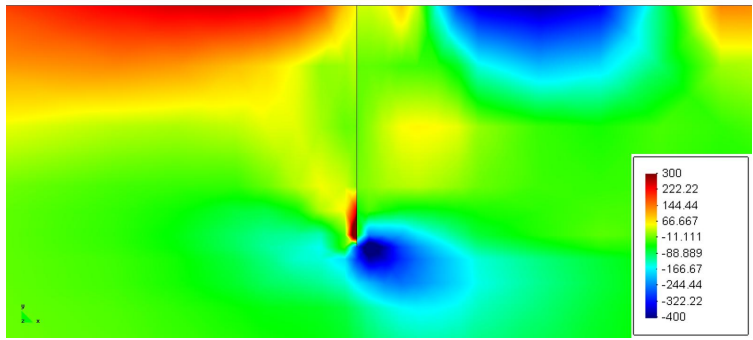


c

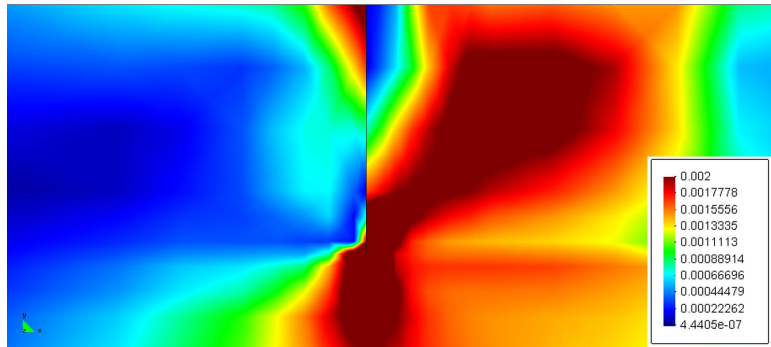


d

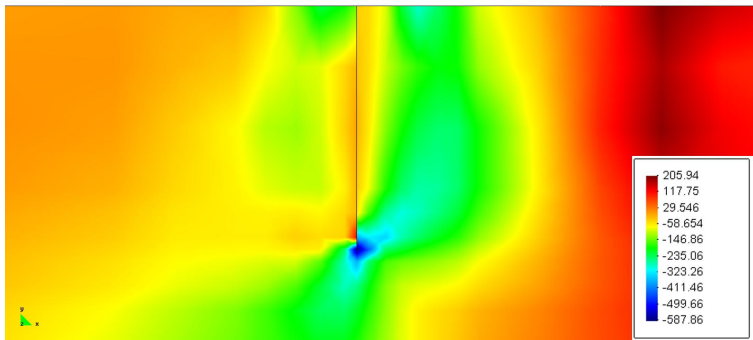
Fig. 4.1



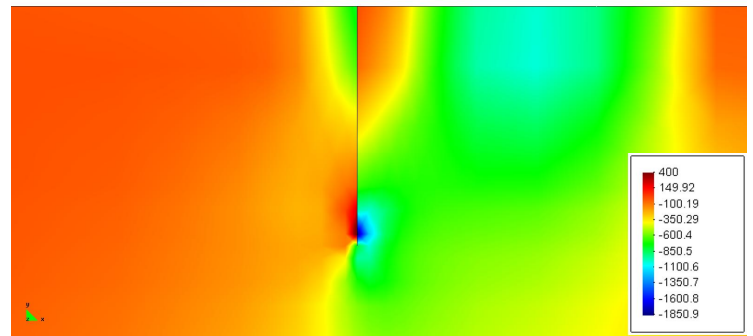
a



b

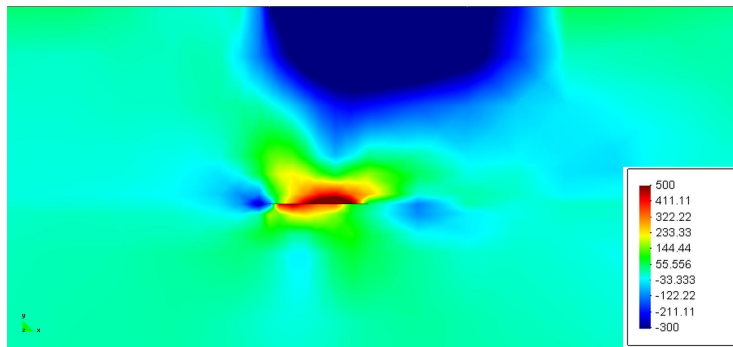


c

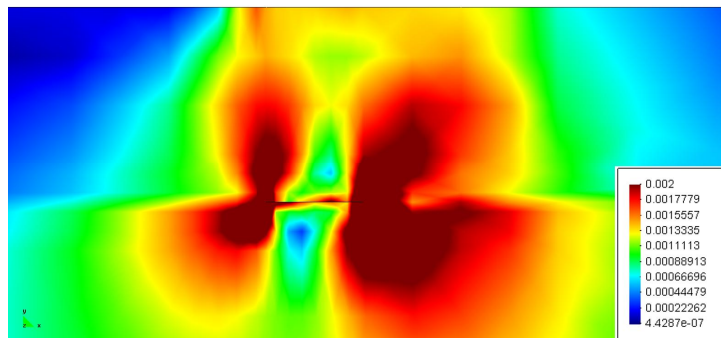


d

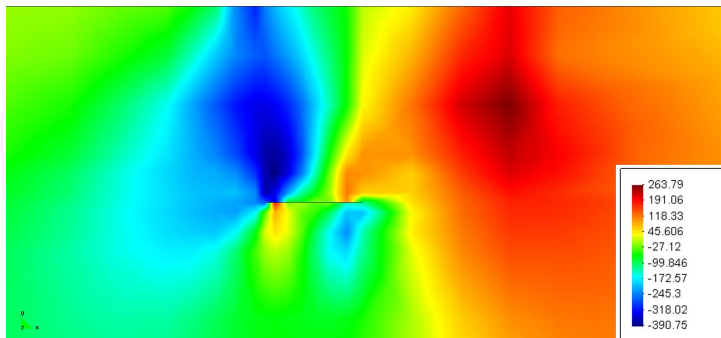
Fig. 4.2



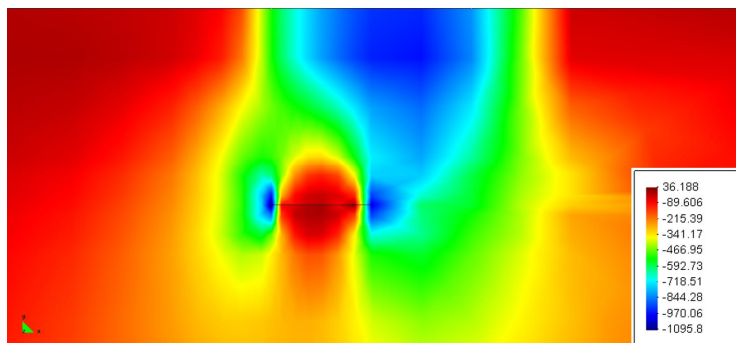
a



b

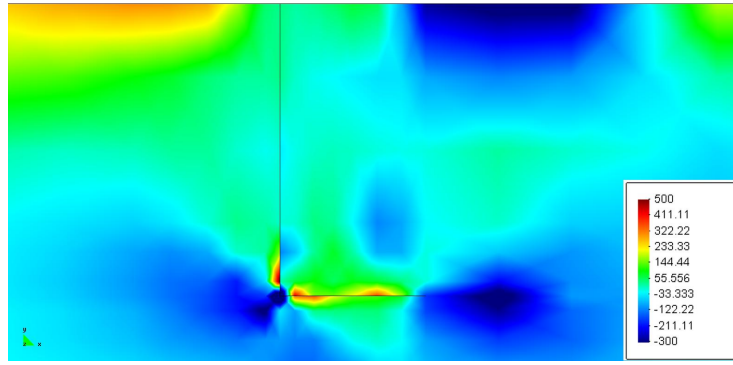


c

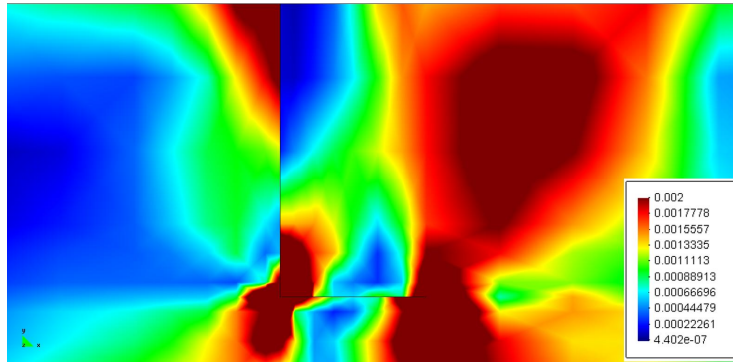


d

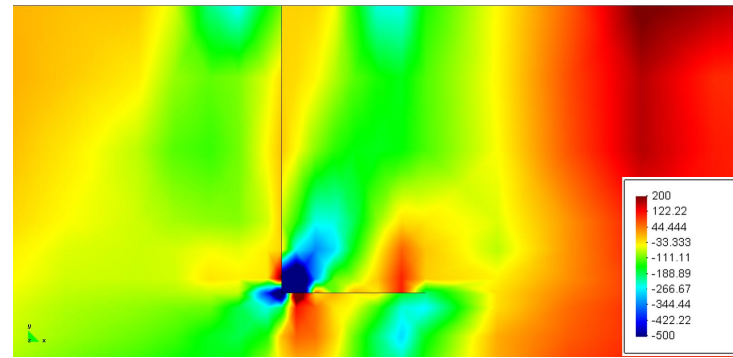
Fig. 4.3



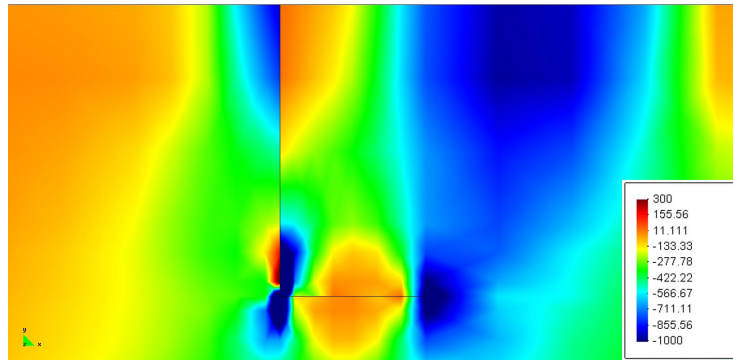
a



b

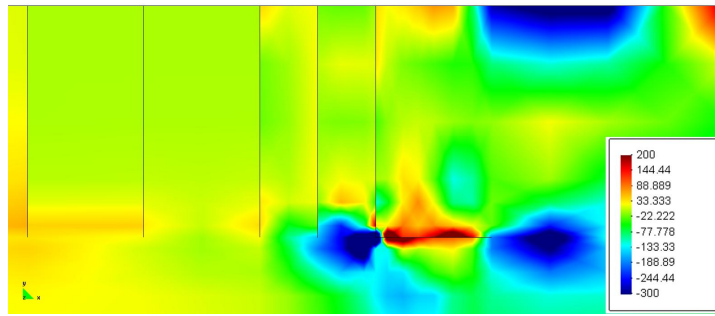


c

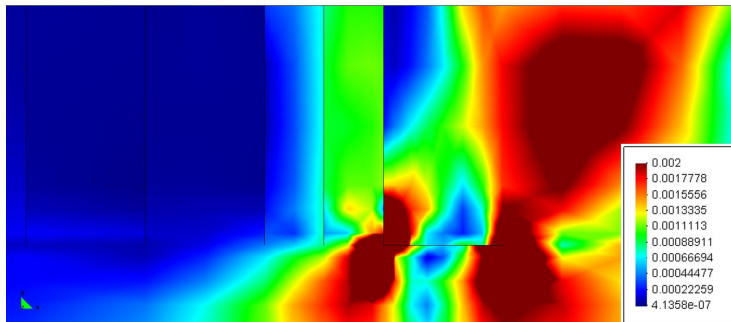


d

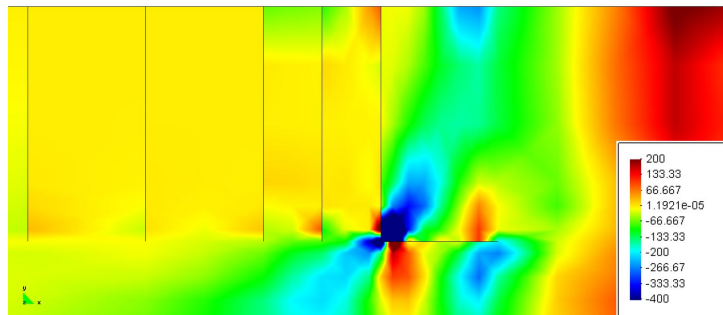
Fig. 4.4



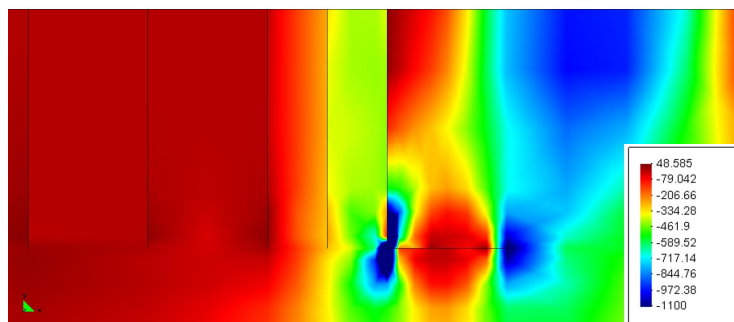
a



b



c



d

Fig. 4.5